NASA TECHNICAL MEMORANDUM

NASA TM X-3028

NASA TM X-3028

PRESSURE-LOSS AND FLOW COEFFICIENTS INSIDE A CHORDWISE-FINNED, IMPINGEMENT, CONVECTION, AND FILM AIR-COOLED TURBINE VANE

by Steven A. Hippensteele

Lewis Research Center
Cleveland, Ohio 44135

NATIONAL AERONAUTICS AND SPACE ADMINISTRATION • WASHINGTON, D. C. • APRIL 1974

1. Report No.	2. Government Accession No.	3. Recipient's Catalog No.
NASA TM X-3028		

4. Title and Subtitle	5. Report Date
PRESSURE-LOSS AND FLOW COEFFICIENTS INSIDE A CHORDWISE-FINNED, IMPINGEMENT, CONVECTION, AND FILM AIR-COOLED TURBINE VANE	APRIL 1974
	6. Performing Organization Code

7. Author(s)	8. Performing Organization Report No.
Steven A. Hippensteele	E-7719
	10. Work Unit No. 501-24

9. Performing Organization Name and Address	11. Contract or Grant No.
Lewis Research Center National Aeronautics and Space Administration Cleveland, Ohio 44135	
	13. Type of Report and Period Covered
12. Sponsoring Agency Name and Address	Technical Memorandum
National Aeronautics and Space Administration Washington, D.C. 20546	14. Sponsoring Agency Code

15. Supplementary Notes

16. Abstract

Total-pressure-loss coefficients, flow discharge coefficients, and friction factors were determined experimentally for the various area and geometry changes and flow passages within an air-cooled turbine vane. The results are compared with those of others obtained on similar configurations, both actual and large models, of vane passages. The supply and exit air pressures were controlled and varied. The investigation was conducted with essentially ambient-temperature air and without external flow of air over the vane.

17. Key Words (Suggested by Author(s))	18. Distribution Statement
Turbine cooling Flow distribution Pressure distribution Impingement cooling Film cooling Convection cooling	Unclassified-unlimited Category 01 CAT.01

19. Security Classif. (of this report)	20. Security Classif. (of this page)	21. No. of Pages	22. Price*
Unclassified	Unclassified	27	$3.25

* For sale by the National Technical Information Service, Springfield, Virginia 22151

PRESSURE-LOSS AND FLOW COEFFICIENTS INSIDE A CHORDWISE-FINNED, IMPINGEMENT, CONVECTION, AND FILM AIR-COOLED TURBINE VANE

by Steven A. Hippensteele

Lewis Research Center

SUMMARY

Total-pressure-loss coefficients, flow discharge coefficients, and friction factors were experimentally determined for the various area and geometry changes and flow passages within an air-cooled turbine vane. The supply and local external pressure levels of the vane, with no external flow of gas over the airfoil, were controlled to simulate those which might be expected in an engine. The investigation was conducted with essentially ambient-temperature air. The measured expansion and contraction total-pressure-loss coefficients ranged from 1.03 to 1.85. These coefficients in general can be predicted within about 20 percent with available information. The orifice flow discharge coefficients were essentially constant and varied from 0.73 to 0.87. These values compared well with results that others obtained with similar passage configurations.

INTRODUCTION

An experimental investigation was made to determine total-pressure-loss coefficients, flow discharge coefficients, and friction factors of an air-cooled turbine vane and to compare the results with available data or correlations.

An accurate knowledge of cooling airflow distribution within turbine vanes is necessary for the correct prediction of both metal temperature distribution and vane life. Cooling airflow distribution is, in turn, based on accurate knowledge of pressure-loss and flow coefficients. This study is part of a series of studies by the Lewis Research Center to investigate experimental coolant pressure-loss and flow coefficients in various vanes, blades, and flow models. In a previous study (ref. 1), the discharge coefficients for thick-plate orifice flow models were determined. In reference 2 the coolant flow through a predominantly convection-cooled vane with trailing-edge pin fins and leading-edge impingement cooling was

investigated. Reference 3 investigated the flow characteristics of several turbine airfoil cooling system configurations consisting of leading-edge impingement, impingement with crossflow, pin fins, a feeder supply tube, and a composite model. An analysis of pressure and flow distribution in a strut-supported wire-cloth vane was made in reference 4. The present report covers the experimental determination of total-pressure-loss coefficients in a vane inlet and airfoil section, flow discharge coefficients in impingement and film cooling holes, and friction factors in chordwise fin cooling passages.

The experimental tests were conducted on a full-size convection- and film-cooled test vane with a 9.8-centimeter (3.86-in.) span and a 6.1-centimeter (2.4-in.) chord. Collectors were attached to the film-cooling and trailing-edge discharge ports, and the collector pressures were controlled to simulate the external pressure distribution experienced in turbine operation. The tests were run with air temperatures of 300 K (80° F) and pressures of about 2 to 3 atmospheres.

In the vane design studied, a portion of the supply air impinged on the leading edge and then exited through film cooling holes on both the suction and pressure surfaces. The remaining cooling air flowed through chordwise fin passages in the midchord region and then exited through a split trailing edge.

APPARATUS

Test Equipment

The flow measuring and distribution equipment used is shown schematically in figure 1. Air at 86.2 N/cm^2 (125 psig) entered the test equipment, was dried and filtered, and passed through a pressure regulator to the test vane. The air that exited from openings in the vane suction side, pressure side, and trailing edge was ducted to separate collectors attached as shown in figure 2. From the collectors the air passed through separate flowmeters and throttling valves before being discharged to the atmosphere. The collectors were closed-end steel cylinders with contoured slots. These collectors were attached by screws to the vane and sealed with an air-curing silicone.

Test Vane

A sectioned view of the chordwise-finned air-cooled test vane with its suction- and pressure-side film cooling holes and split trailing edge is shown in figure 3. The vane span is 9.8 centimeters (3.86 in.), and the chord is 6.1 centimeters (2.4 in.). Air enters from an inlet tube at the top and flows through a tip chamber into a plenum at the midchord of the airfoil, as shown in figure 4. From there the flow divides into three parts. The first part flows through a row of 46 impingement holes, each 0.127 centimeter (0.050 in.) in diameter, impinges on the leading edge, and exits through film cooling holes on both the suction and pressure sides. The suction side has a row of 59 holes that are each 0.064 centimeter (0.025 in.) in diameter, and the pressure side has rows of 58 and 59 holes that are each 0.071 centimeter (0.028 in.) in diameter. The second and third parts of the airflow from the midchord plenum enter the 92 suction-side and 92 pressure-side chordwise fin cooling passages and then recombine to exit through the 0.072 centimeter (0.028 in.) wide split trailing edge.

Instrumentation

Flow. - The airflows into the test vane and out of the three collectors were separately measured by commercial flowmeters (rotameters) with an accuracy of ½ percent of full scale.

Pressure. - The pressures in the vane and collectors were measured with 31 static-pressure taps. The air inlet static pressure was measured by a tap in the supply tube (location I in fig. 4). The air exit static pressures were measured by taps in each of the three collectors. The locations for the taps in the collectors at the suction-side, pressure-side, and trailing-edge exits are shown in figure 2 and designated as S, P, T, respectively. Nine static-pressure taps were located in the airfoil section at each of three spanwise positions shown in figure 4: 1.6 centimeters (0.63 in.) from the tip platform, 4.9 centimeters (1.93 in.) from the tip platform, and 1.6 centimeters (0.63 in.) from the hub platform. Pressure taps were designated by numbers 1 to 9 (fig. 2) located at each of the tip, midspan, and hub locations. These taps measured the pressure at the central plenum (1), the downstream side of the leading-edge

impingement holes (2), the upstream side of the suction-side (3) and pressure-side (4) film cooling holes, the entrance (5) and exit (6) of the suction-side cooling fin passages, the entrance (7) and exit (8) of the pressure-side cooling fin passages, and the entrance to the trailing edge (9). Although read independently, the pressures from each of the three span locations were mathematically averaged for calculations. The pressures were measured on Bourdon-type pressure gages and water U-tubes. Measured pressures were accurate to within ± 0.034 N/cm^2 (0.05 psi).

Temperature. - The inlet air temperature was measured at the same locations as the inlet pressure (location I, fig. 4) by a Chromel-Alumel thermocouple. The temperature of the air from each of the three exits from each of the three exits from the vane was measured by a Chromel-Alumel thermocouple in each collector. The temperature measurements were read on a null balance potentiometer.

EXPERIMENTAL PROCEDURE

In the first set of tests the inlet pressure to the test vane was varied over several different values [from 21.0 to 23.5 N/cm^2 (30.5 to 33.8 psia)] while the three exit pressures (suction, pressure, and trailing edge) remained constant at 20.7 N/cm^2 (30.0 psia). In the second set of tests the inlet pressure to the test vane remained constant at several different values [from 22.8 to 30.3 N/cm^2 (33.0 to 44.0 psia)] while each of the three exit pressures was varied independently over a range of pressures. Two pressures were maintained at nominal while the third was varied from minimum measurable airflow to maximum airflow. In the third set of tests the inlet pressure to the test vane was varied over several different values [from 28.4 to 31.9 N/cm^2 (41.2 to 46.2 psia)] while the three exit pressures (suction, pressure, and trailing edge) remained constant at what was considered to be the design pressure distribution around the vane, [22.8, 27.6, and 20.7 N/cm^2 (33.0, 40.0, and 30.0 psia)], respectively.

The four temperatures, the 31 pressures, the inlet flow, and the three exit flows were measured and recorded for each of the 75 test runs made. The conditions for the test runs are summarized in table I.

ANALYTICAL PROCEDURE

The analysis to determine the correlations for the experimental pressure-loss data and to predict loss coefficients for the airflow within the test vane required some simplifying assumptions. It should be recognized that the ideal method for determining the correlations would be to measure flows and pressures at many spanwise positions. However, that detail is beyond the scope of these tests. A discussion of the analytical methods and assumptions follows.

Vane Inlet Overall Loss Coefficient

Starting at the vane inlet, there is a sudden expansion from the circular passage (location I), as shown in figure 4, to a parallel, pipe-shaped tip chamber (location Ia). Then there is a contraction from this tip chamber as the air enters the airfoil portion of the vane (location Ib). We assume incompressible flow in the low-Mach-number region between these locations. Thus, the total-pressure losses for the expansion and contraction (using the symbols defined in the appendix) can be written, respectively, as

$$P_I - P_{Ia} = K_E \frac{\rho_I V_I^2}{2g_c} \tag{1}$$

and

$$P_{Ia} - P_{Ib} = K_C \frac{\rho_I V_I^2}{2g_c} \tag{2}$$

The individual losses were not determined for the test vane since a static tap was not located in the tip chamber at location Ia. Instead, overall losses between stations I and Ib were determined. To analytically evaluate an overall loss coefficient for these regions combined, equations (1) and (2) are combined to give

$$P_I - P_{Ib} = K_E \frac{\rho_I V_I^2}{2g_c} + K_C \frac{\rho_{Ib} V_{Ib}^2}{2g_c} \tag{3}$$

Simplifying and solving for an overall loss coefficient K_{OI} yield

$$K_{OI} = \frac{P_I - P_{Ib}}{\frac{\rho_I V_I^2}{2g_c}} \tag{4}$$

where

$$K_{OI} = K_E + K_C \frac{\rho_{Ib} V_{Ib}^2}{\rho_I V_I^2} \tag{5}$$

The experimental inlet overall total-pressure-loss coefficient was determined from measured values of p_I, p_{Ib}, T_I, and W_I by the use of the equation of state, the continuity equation, and the Bernoulli equation. These gave the necessary terms for location I (and similarly for location Ib) in (4) and (5):

$$\rho_I = \frac{p_I}{RT_I} \tag{6}$$

$$V_I = \frac{W_I}{\rho_I A_I} \tag{7}$$

and

$$P_I = p_I + \frac{\rho_I V_I^2}{2g_c} \tag{8}$$

By using the flow area changes that existed in the test vane, an expansion loss K_E and a contraction loss K_C can be determined from the analysis in reference 5. Combining the values of these coefficients with the ρV^2 ratios at locations I and Ib and using measured pressures as in equation (5) will give an analytically predicted inlet overall loss coefficient.

Airfoil Leading Edge

Impingement-hole discharge coefficient. - The airflow after entering the airfoil plenum flows through 46 holes of 0.127-centimeter (0.050-in.) diameter in a 0.127-centimeter (0.050-in.) thick insert to impingement cool the leading edge. To predict the actual flow through the openings, a flow discharge coefficient C_D is needed. This coefficient relates actual flow

to ideal flow and was determined from experimental data by using the equation

$$C_{D,H} = \frac{W_H}{\rho_H A_H V_H} \tag{9}$$

where W_H is measured and ρ_H and V_H can be calculated from relations of compressible flow

$$\rho_H = \frac{p_2}{RT}\left(\frac{P_1}{p_2}\right)^{(\gamma-1)/\gamma} \tag{10}$$

and

$$V_H = \sqrt{\frac{2\gamma g_c RT}{\gamma - 1}\left[1 - \left(\frac{p_2}{P_1}\right)^{(\gamma-1)/\gamma}\right]} \tag{11}$$

where C_D is a function of flow Reynolds number $WD/A\mu$. Generally, C_D increases with Reynolds number at low values of Reynolds number, but becomes constant at high values (ref. 1). The discharge coefficients determined in this report are plotted against Reynolds number.

Overall loss coefficient. - In addition to the determination of the impingement-hole flow discharge coefficient $C_{D,H}$, an overall total-pressure-loss coefficient was determined that included losses in the flow from the central plenum after it passed through the impingement holes and around the leading-edge interior and before it exited out of the film-cooling holes. This overall loss coefficient based on compressible flow equations (4), (10), and (11) combines expansion, turning, and contraction losses. For the suction side, equation (4) becomes

$$K_{OL,S} = \frac{P_1 - P_3}{\frac{\rho_H V_H^2}{2g_c}} \tag{12}$$

and, for the pressure side,

$$K_{OL,P} = \frac{P_1 - P_4}{\frac{\rho_H V_H^2}{2g_c}} \tag{13}$$

where ρ_H and V_H were found by using equations (10) and (11), respectively.

Film-cooling-hole discharge coefficients. - After the air flows around the leading edge, it exits through a row of fifty-nine 0.064-centimeter (0.025-in.) diameter holes in the suction side and rows of fifty-eight and fifty-nine 0.071-centimeter (0.028-in.) diameter holes in the pressure side. For the suction side the flow discharge coefficient $C_{D,S}$ is determined by using equations (9) to (11) but with subscripts S, 3, and S substituted for H, 1, and 2, respectively, in these equations. For the pressure-side coefficient $C_{D,P}$, subscripts P, 4, and P are substituted for H, 1, and 2, respectively, in these equations. The discharge coefficients are plotted against Reynolds number.

Airfoil Midchord

Fin-passage friction factors. - Fanning friction factors for the suction- and pressure-side fin passages can be determined, assuming only viscous losses through the passages. The Fanning friction factor (ref. 6) of the fin passages was determined for the suction side by using

$$f_{FS} = \frac{P_5 - P_6}{\frac{\rho_{FS} V_{FS}^2}{2g_c}} \left(\frac{D_{FS}}{4L_{FS}} \right) \tag{14}$$

and for the pressure side by using

$$f_{FP} = \frac{P_7 - P_8}{\frac{\rho_{FP} V_{FP}^2}{2g_c}} \left(\frac{D_{FP}}{4L_{FP}} \right) \tag{15}$$

The densities were obtained from the equation of state. The passage velocities were obtained from the continuity equation [eq. (7)]. This, however, required that the flow split between the suction- and pressure-side fin passages be known. To obtain the flow W_{FS} through the suction-side fin passage, assume that the values of pressure drop, friction factor, cross-sectional area, hydraulic diameter, and density are the same for both the suction and pressure cooling fin passages. Starting with

$$\Delta P_{FS} = \Delta P_{FP}$$

$$\frac{2f_{FS}}{g_c \rho_{FS}} \left(\frac{W_{FS}}{A_{FS}} \right)^2 \frac{L_{FS}}{D_{FS}} = \frac{2f_{FP}}{g_c \rho_{FP}} \left(\frac{W_{FP}}{A_{FP}} \right)^2 \frac{L_{FP}}{D_{FP}}$$

$$W_{FS}^2 L_{FS} = W_{FP}^2 L_{FP}$$

and noting that the flow through the 92 suction-side and 92 pressure-side chordwise fin cooling passage is

$$92W_{FS} + 92W_{FP} = W_T \tag{16}$$

yields

$$W_{FS} = \frac{W_T}{92 \left(1 + \sqrt{\frac{L_{FS}}{L_{FP}}} \right)} \tag{17}$$

The flow through the pressure-side passages was obtained by subtracting the total suction-side flow from the total measured trailing-edge flow. Friction factors were plotted against Reynolds number.

Fin-passage expansion loss coefficients. - Expansion total-pressure-loss coefficients were determined for the flow out of the suction- and pressure-side cooling fin passages by applying equation (4), with subscripts changed to give

$$K_{FS} = \frac{P_6 - P_9}{\frac{\rho_6 V_6^2}{2g_c}} \tag{18}$$

for the suction-side fin-passage outlets and

$$K_{FP} = \frac{P_8 - P_9}{\frac{\rho_8 V_8^2}{2g_c}} \tag{19}$$

for the pressure-side fin-passage outlets. The velocities and densities can be obtained by using the flow split equation (16) and the state, continuity, and the Bernoulli equations. By using the area changes that exist loss coefficients can be estimated from the analysis in reference 7.

Airfoil Trailing-Edge Discharge Coefficient

After the flow passes out of the midchord cooling fin passages, it flows through a 0.071-centimeter (0.028-in.) wide trailing-edge passage. A flow discharge coefficient is needed to predict the actual flow through the trailing-edge passage. This coefficient was determined from experimental data by using equations (9) to (11) but with the subscripts H, 1, and 2 changed to TE, 9, and T, respectively. The trailing-edge flow discharge coefficient $C_{D,TE}$ is plotted against Reynolds number.

RESULTS AND DISCUSSION

Vane Inlet Overall Loss Coefficient

An overall total-pressure-loss coefficient based on the total-pressure difference between locations I and Ib and the area at location I was determined. Separate experimental expansion and contraction loss coefficients between these locations could not be determined because there was no pressure tap at location Ia. The experimental inlet overall loss coefficient K_{OI} was determined by using equations (4) to (8). The coefficient is the slope of the plot of the total-pressure difference against the velocity head shown in figure 5. For the majority of the data the average value is 1.50, which except for group 6 (table I), is correlated within 22 percent. Using the flow area ratio of location I to Ia and location Ia to Ib and the data of reference 5 combined with equation (5) gives an analytical prediction of K_{OI} of 1.2. The higher value obtained in actual tests on the airfoil would be expected because of the more complex geometry of the actual vane compared to that assumed in reference 5. The reason for the departure of group 6 data was not apparent.

Airfoil Leading Edge

Impingement-hole discharge coefficient. - The compressible flow discharge coefficient $C_{D,H}$ based on measured flows and the pressures at locations 1 and 2 obtained by using equations (9) to (11) is shown in figure 6. The data indicate an essentially constant coefficient of 0.74 (within 4 percent for the majority of the data). This value agrees with the experimental value of 0.79 from reference 3 for a similar configuration and conditions.

Overall loss coefficient.- The overall total-pressure-loss coefficients for the suction side $K_{OL,S}$ and the pressure side $K_{OL,P}$ were determined by using measured flows and pressures at locations 1, 3 (for suction side), and 4 (for pressure side) and equations (10) to (13). The coefficients for the suction and pressure sides, shown in figures 7 (a) and (b), respectively, are the slope of the plot of the total-pressure difference against the velocity head. The majority of the data correlated within 10 percent of a value of 1.03 for both suction and pressure sides. Reference 3 investigated a similar configuration with the same ratio of hole diameter to impingement-wall distance and the same range of impingement-hole flow Mach numbers and obtained the following correction:

$$K_{OL} = 0.972 + 0.465\, M_H^2$$

This correlation gives an average value of 1.02 for the conditions presented in the report, which agrees closely with the value of 1.03 obtained in the test.

Film-cooling-hole discharge coefficients. - The compressible flow discharge coefficients for the suction side $C_{D,S}$ and for the pressure side $C_{D,P}$ based on measured flows and pressures at locations 3 and S for the suction side and 4 and P for the pressure side, are shown in figures 8(a) and (b), respectively. The data indicate that both coefficients are essentially constant, $C_{D,S}$ at 0.78 (within 4 percent) and $C_{D,P}$ at 0.73 (within 6 percent). The reason for the difference in coefficients is not apparent. However, it should be noted that the pressure side has two rows of film cooling holes and the suction side has only one row, and that the holes on the two sides have slightly different diameters and lengths.

Based on the results of reference 8 and unpublished data, it is expected that the discharge coefficients reported herein would also be a

function of external gas flow over the vane.

Airfoil Midchord

At given pressure tap locations in the midchord fin cooling passages, the spanwise pressures (hub, midspan, and tip) differed by a significant amount when compared with the chordwise pressure drops through the fin passages. The differences in the spanwise pressures indicated the possibility of a spanwise flow variation, for which the exact measurement was beyond the scope of these tests. However, two methods of calculating the spanwise flows were tried. The first was based on a one-dimensional momentum-flow analysis (ref.2) in which part of the vane inlet flow passed out through the impingement holes and fin cooling passages as it flowed from the vane inlet toward the vane hub. The flow analysis utilized the measured inlet flow and the three measured spanwise pressures at location 1. The second method was based on the assumption that each of the cooling-fin-passage entrance-loss coefficients was the same, which then determined the necessary flow at the spanwise locations. Unfortunately, both of these methods gave inconsistent results. Therefore, the three spanwise pressures at each of the chordwise pressure tap locations were averaged for calculating the various coefficients. Entrance-loss coefficients into the fin cooling passages, even when based on average pressures and flows, were found to have values between 0.5 and 4.5. Since these values cannot be explained, they are omitted.

Fin-passage friction factors.- Fanning friction factors for the suction- and pressure-side fin passages were calculated from equations (14) and (15), respectively. The fin-passage flows were determined from equations (16) and (17), where the lengths of the suction-side L_{FS} and pressure-side L_{FP} passages were 1.60 and 1.12 centimeters (0.63 and 0.44 in.), respectively. The suction-side flow was determined to be 45.5 percent of the total trailing-edge flow, with the remainder being the flow through the pressure side. The friction factor data are plotted against passage Reynolds number, with hydraulic diameter taken as the characteristic length dimension, in figures 9 (a) and (b) for the suction- and pressure-side passages, respectively. The laminar-flow friction factor line for square passages (ref. 9) is shown in the figure. In the laminar-flow region, where the Reynolds numbers are between 1000

and 2000, the data fall above the laminar-flow line. In the region of transition to turbulent flow, where the Reynolds numbers are between 3000 and 10 000, the data fall below the Blasius line for circular smooth tubes. Experimental friction factors (ref. 9) fall on the laminar-flow line (Re < 2000) and on or above the Blasius smooth-tube line (Re > 3000), unlike the data presented herein. In reference 10, for a large isosceles triangular passage with a small apex angle, the data exhibited the same tendency as the data presented herein. This reference suggested that, for noncircular passages not flowing full, the transition process is a gradual one, with the turbulent flow appearing first in the passage center and filling more and more of the passage as the Reynolds number increases. Figure 9 shows that using the Blasius formula (ref. 6) provides a conservative estimate of the friction factors for most of the range of Reynolds numbers investigated (3000 to 10 000).

Fin-passage expansion loss coefficients. - The fin-passage expansion total-pressure-loss coefficients were based on measured pressures at locations 6 and 9 for the suction side and at locations 8 and 9 for the pressure side. Flows were determined by using the flow split equation (16). The expansion loss coefficients K_{FS} and K_{FP} were determined from the experimental data by using equations (18) and (19), respectively. They are shown in figures 10 (a) and (b), respectively, as the slope of the plot of the total-pressure difference against the velocity head. The coefficient for the suction side was 1.85 and that for the pressure side was 1.35. These experimental loss coefficients were considerably higher than was expected from the data given in reference 7. This difference most likely results from the differences between the geometries of the vane airfoil used for these tests and the idealized tube flow used to obtain the data of reference 7.

Airfoil Trailing-Edge Discharge Coefficient

The compressible trailing-edge flow discharge coefficient $C_{D,TE}$ based on measured flows and the pressures at locations 9 and T obtained by using equations (9) to (11) is shown in figure 11. The data indicate an essentially constant coefficient of 0.87 (within 2 percent for the majority of the data). In the range of Reynolds numbers tested it is expected, based on unpublished experimental data, that the influence of external gas flow over the vane will have a small effect on the discharge coefficient.

SUMMARY OF RESULTS

A study was conducted to measure coolant flow loss coefficients and friction factors at various locations in a turbine vane cooled by a combination of convection, impingement, and film-cooling methods. Determined were entrance and exit total-pressure-loss coefficients, flow discharge coefficients, and friction factors.

The results of this study are summarized as follows:

1. The expansion and overall total-pressure-loss coefficients which range between 1.03 to 1.85 can be analytically predicted with available information within about 20 percent. The exception was for the expansion coefficient at the outlet of the fin cooling passages, in which case the experimental losses were considerably higher than expected because of mixing losses.

2. The flow discharge coefficients for impingement, film cooling, and trailing-edge passages, which ranged between 0.73 and 0.87, agreed with the experimental results of others. It is expected that the flow discharge coefficients measured would be influenced by external gas flow over the vane.

3. The friction factors in the region of transition to turbulent flow for the range of coolant flow Reynolds numbers investigated fell below the Blasius formula for circular smooth tubes (as do the data of Eckert and Irvine). Thus, the transition to turbulent flow in the fin passages may be gradual. The data indicate that the Blasius formula would provide a conservative estimate of the friction factor.

Lewis Research Center,
National Aeronautics and Space Administration,
Cleveland, Ohio, November 21, 1973,
501-24.

APPENDIX-SYMBOLS

A	area
C_D	flow discharge coefficient
D	hydraulic diameter
f	Fanning friction factor
g_c	gravitational dimension constant
K	total-pressure-loss coefficient
L	length of passage between stations
M	Mach number
P	total pressure
p	static pressure
R	gas constant for air
Re	Reynolds number
T	total temperature
V	average velocity
W	mass flow rate
γ	ratio of specific heats
Δ	difference between two locations
μ	viscosity
ρ	average mass density

Subscripts:

C	vane entrance contraction
E	vane entrance expansion
FP	midchord pressure-side cooling fin passage
FS	midchord suction-side cooling fin passage
H	leading-edge impingement holes
I,Ia, Ib	vane inlet, tip chamber, and airfoil plenum inlet locations

OI	overall vane inlet from location I to location Ib
OL	overall vane leading edge from location 1 to film cooling holes
OL,P	overall vane leading edge from location 1 to location 4
OL,S	overall vane leading edge from location 1 to location 3
P	outside the pressure-side film cooling holes
S	outside the suction-side film cooling holes
T	outside the trailing-edge outlet
TE	inside the trailing-edge outlet
1 to 9	pressure tap locations, each at tip, midspan, and hub

REFERENCES

1. Rohde, John E.; Richards, Hadley T.; and Metger, George W.: Discharge Coefficients for Thick Plate Orifices with Approach Flow Perpendicular and Inclined to the Orifice Axis. NASA TN D-5467, 1969.

2. Clark, John S.; Richards, Hadley T.; Poferl, David J.; and Livingood, John N.B.: Coolant Pressure and Flow Distribution Through an Air-Cooled Vane for a High-Temperature Gas Turbine. NASA TM X-2028, 1970.

3. Damerow, W.P.; Murtaugh, J.P.; Burggraf, F.: Experimental and Analytical Investigation of the Coolant Flow Characteristics in Cooled Turbine Airfoils. Rep. R72AEG165, General Electric Co. (NASA CR-120883), June 1972.

4. Kaufman, Albert; Poferl, David J.; and Richards, Hadley T.: Coolant Pressure and Airflow Distribution in a Strut-Supported Transpiration-Cooled Vane for a Gas Turbine Engine. NASA TN D-6916, 1972.

5. Staff of Engineering Division: Flow of Fluids Through Valves, Fittings, and Pipe. Tech. Paper 410, Crane Co., 1965.

6. Shapiro, Ascher H.: The Dynamics and Thermodynamics of Compressible Fluid Flow. Vol. I. Ronald Press Co., 1953.

7. Kunkle, John S.; Wilson, Samuel D.; and Cota, Richard A.; eds.: Compressed Gas Handbook. NASA SP-3045, 1969.

8. Dewey, Paul E.: A Preliminary Investigation of Aerodynamic Characteristics of Small Inclined Air Outlets at Transonic Mach Numbers. NACA TN 3442, 1955.

9. Schlichting, Hermann; (J. Kestin, trans.): Boundary Layer Theory. Fourth ed., McGraw-Hill Book Co., Inc., 1960.

10. Eckert, E.R.G.; and Irvine, T.F., Jr.: Pressure Drop and Heat Transfer in a Duct with Triangular Cross Section. J. Heat Transfer, vol. 82, no. 2, May 1960, pp. 125-138.

TABLE I. - SUMMARY OF EXPERIMENTAL TEST CONDITIONS

Group	Description	Collector pressures								Flow rate that varied, location-
		Vane inlet, location I		Outside pressure-side film-cooling holes, location P		Outside suction-side film-cooling holes, location S		Outside trailing-edge outlet, location T		
		N/cm^2	Psia	N/cm^2	Psia	N/cm^2	Psia	N/cm^2	Psia	
1	Equal, constant collector pressure	21.0 to 23.5	30.5 to 33.8	20.7	30.0	20.7	30.0	20.7	30.0	I
2	Leading edge at design for engine inlet pressure of 31 N/cm^2 (45 psia) and design pressure outside trailing-edge outlet of 18.6 N/cm^2 (27 psia)	29.0	42.0	27.6	40.1	22.7	32.9	20.8 to 28.3	30.1 to 41.0	T
3	Same as group 2	30.3	44.0	27.6	40.1	22.7	32.9	25.5 to 29.6	37.0 to 43.0	T
4	Leading edge at design for engine inlet pressure of 24 N/cm^2 (35 psia) and design pressure outside trailing-edge outlet of 14.5 N/cm^2 (21 psia)	22.8	33.0	21.5	31.2	17.6	25.5	14.5 to 22.1	21.1 to 32.0	T
5	Same as group 4	24.1	35.0	21.5	31.2	17.6	25.5	16.8 to 23.4	23.7 to 33.9	T
6	Same as group 2, except for design pressure outside suction-side film cooling holes of 22.7 N/cm^2 (32.9 psia)	29.0	42.0	27.6	40.1	18.6 to 27.9	27.0 to 40.4	18.6	27.0	S
7	Same as group 6	30.3	44.0	27.6	40.1	22.7 to 28.8	32.9 to 41.8	18.6	27.0	S
8	Same as group 2, except for design pressure outside pressure-side film cooling holes of 27.6 N/cm^2 (40.1 psia)	29.0	42.0	25.1 to 27.7	36.4 to 40.2	22.7	32.9	18.6	27.0	P
9	Same as group 8	30.3	44.0	26.3 to 29.0	38.1 to 42.0	22.7	32.9	18.6	27.0	P
10	Constant collector pressures	28.4 to 31.9	41.2 to 46.2	27.6	40.0	22.8	33.0	20.7	30.0	I

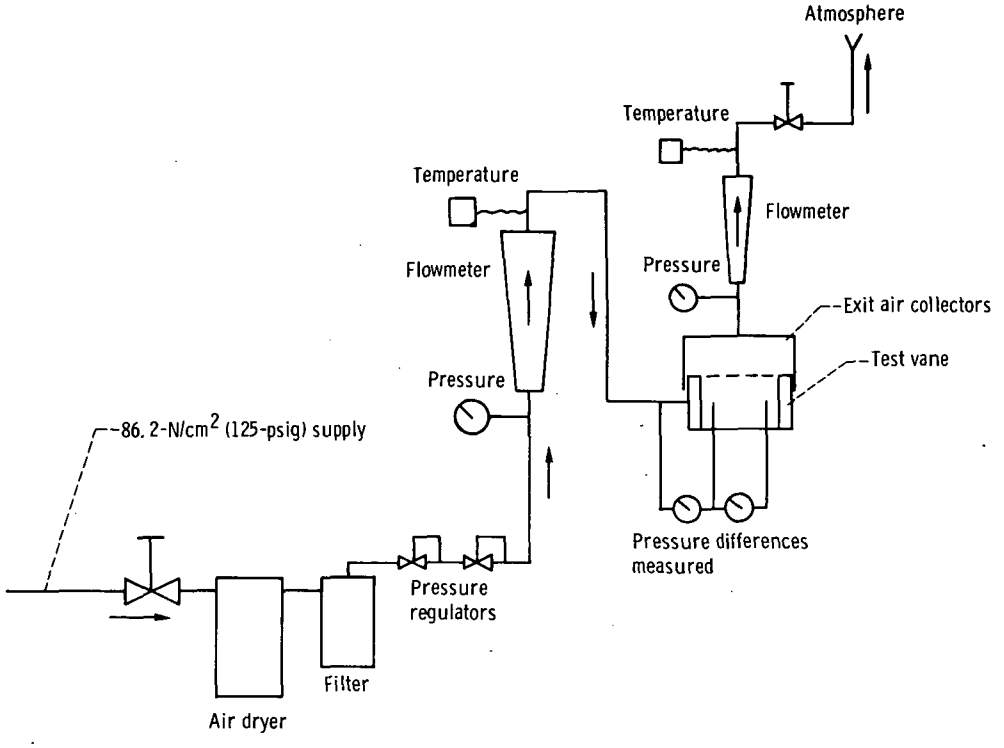

Figure 1. - Flow measuring and distribution equipment.

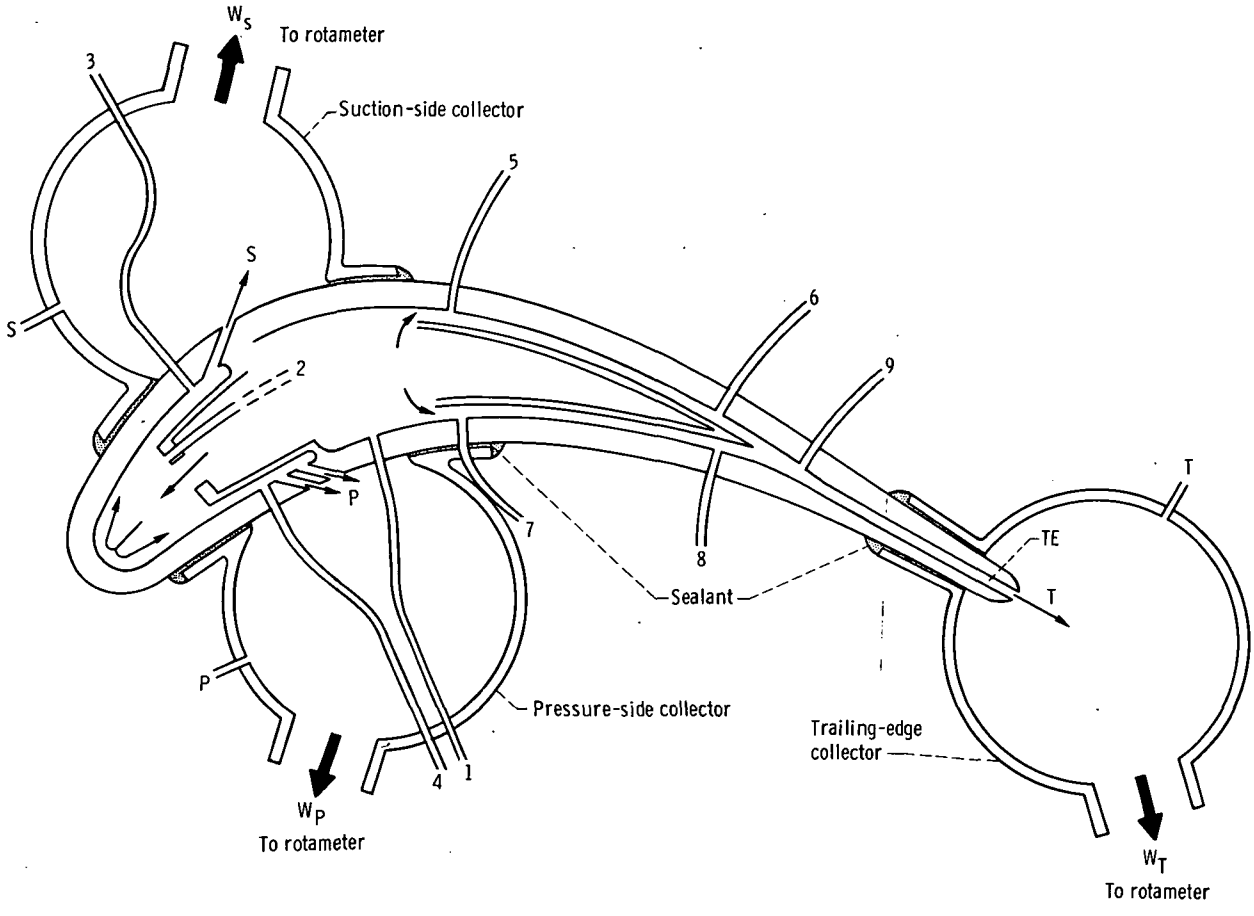

Figure 2. - Air collector and pressure tap locations.

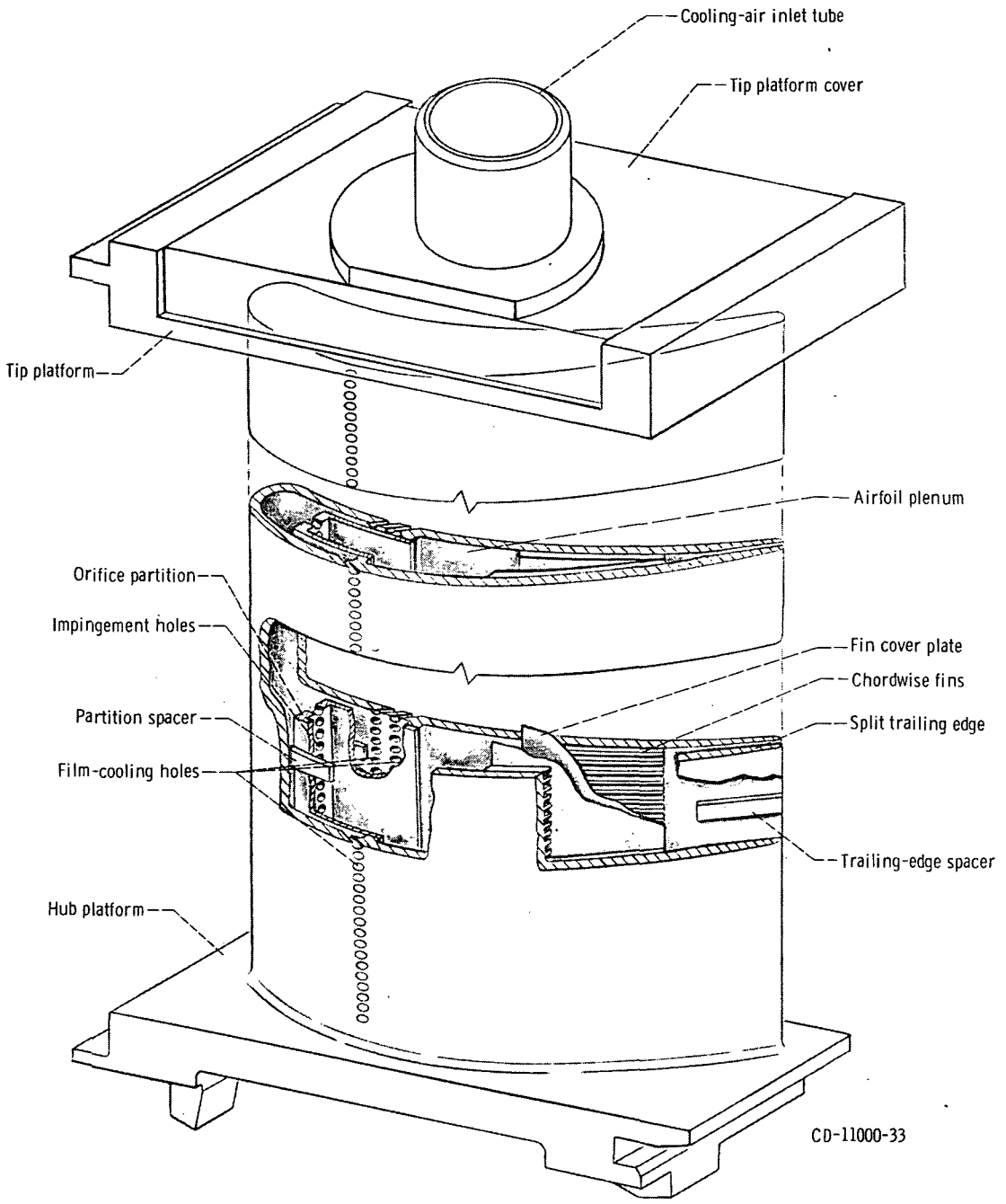

Figure 3. - Test vane (sectioned view).

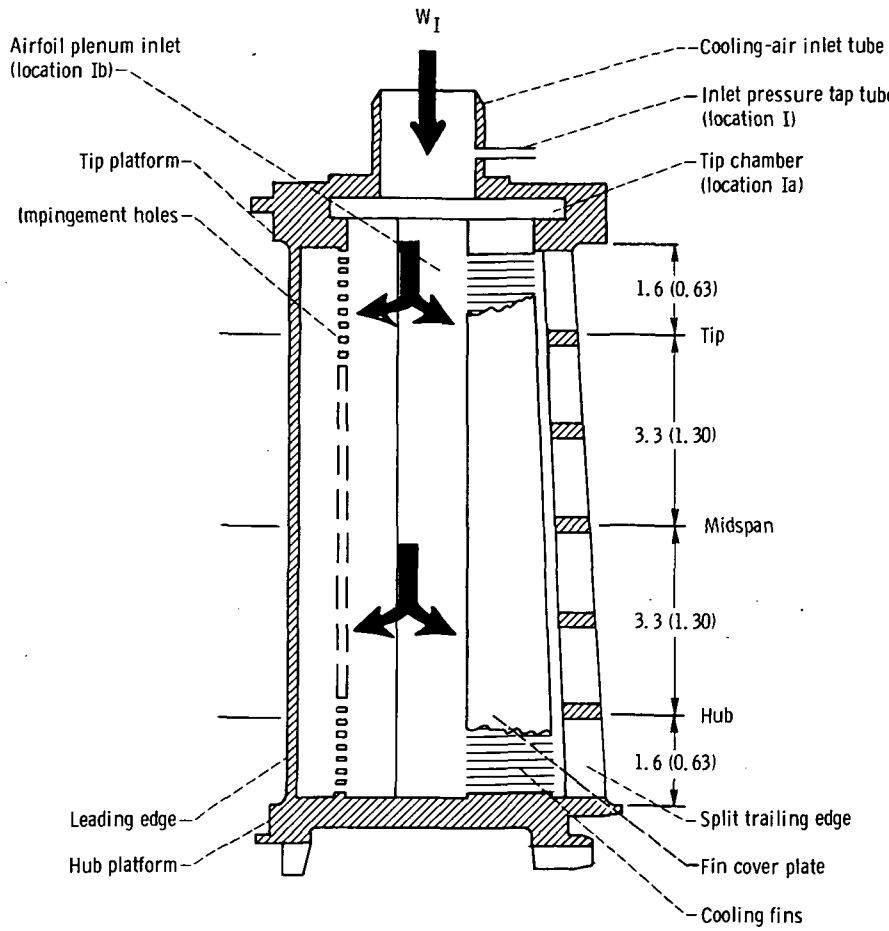

Figure 4. - Test vane instrumentation locations. (Dimensions are in cm (in.).)

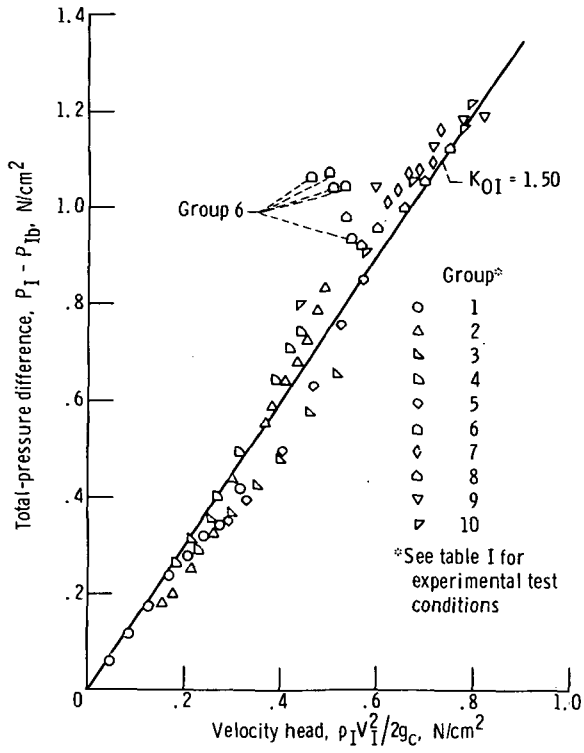

Figure 5. - Vane overall inlet loss coefficient.

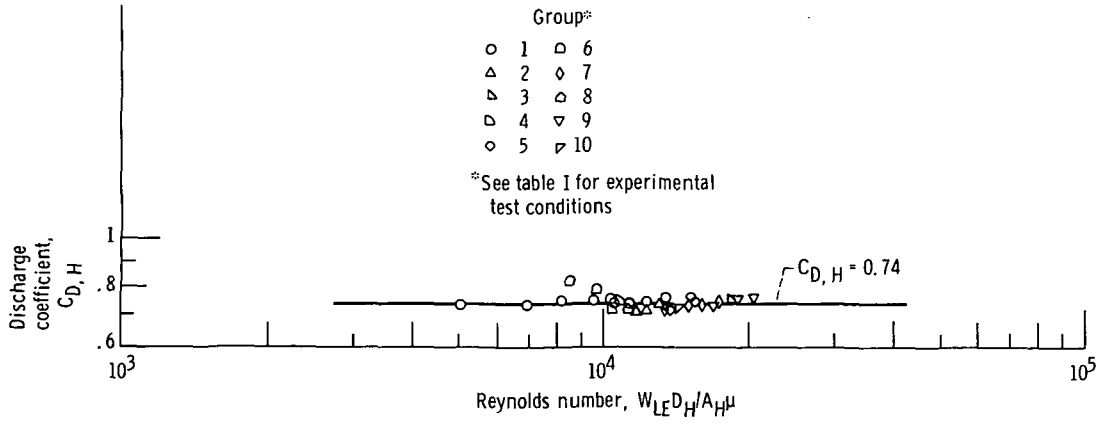

Figure 6. - Discharge coefficient for leading-edge impingement holes as function of Reynolds number.

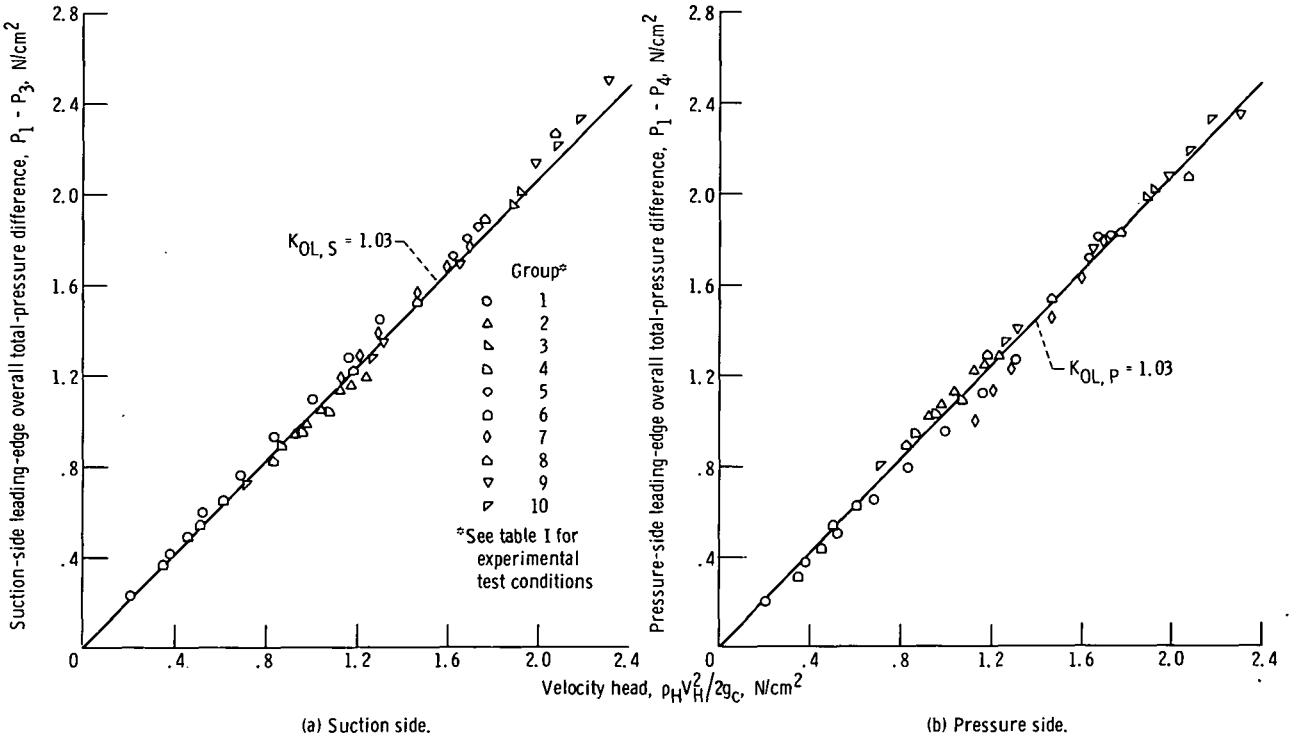

(a) Suction side.

(b) Pressure side.

Figure 7. - Leading-edge overall loss coefficients.

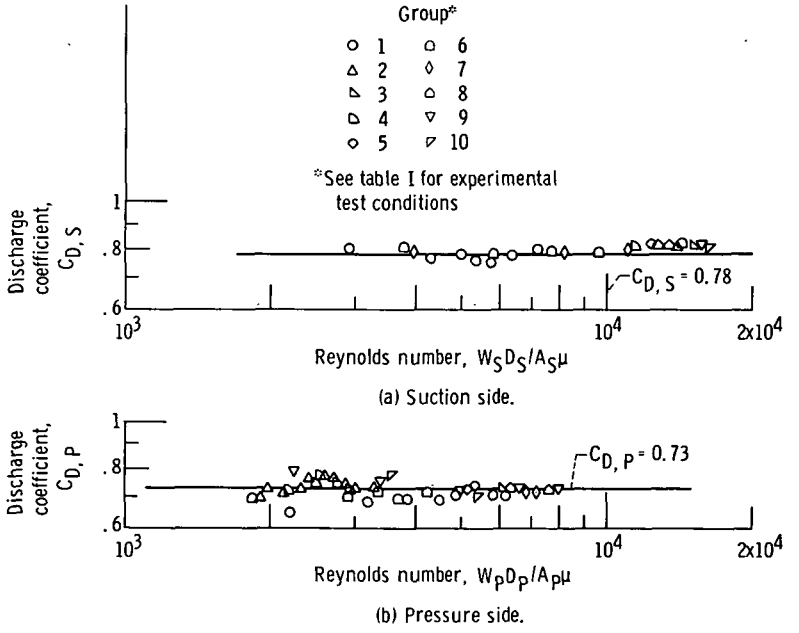

(a) Suction side.

(b) Pressure side.

Figure 8. - Discharge coefficients for film-cooling holes as function of Reynolds number.

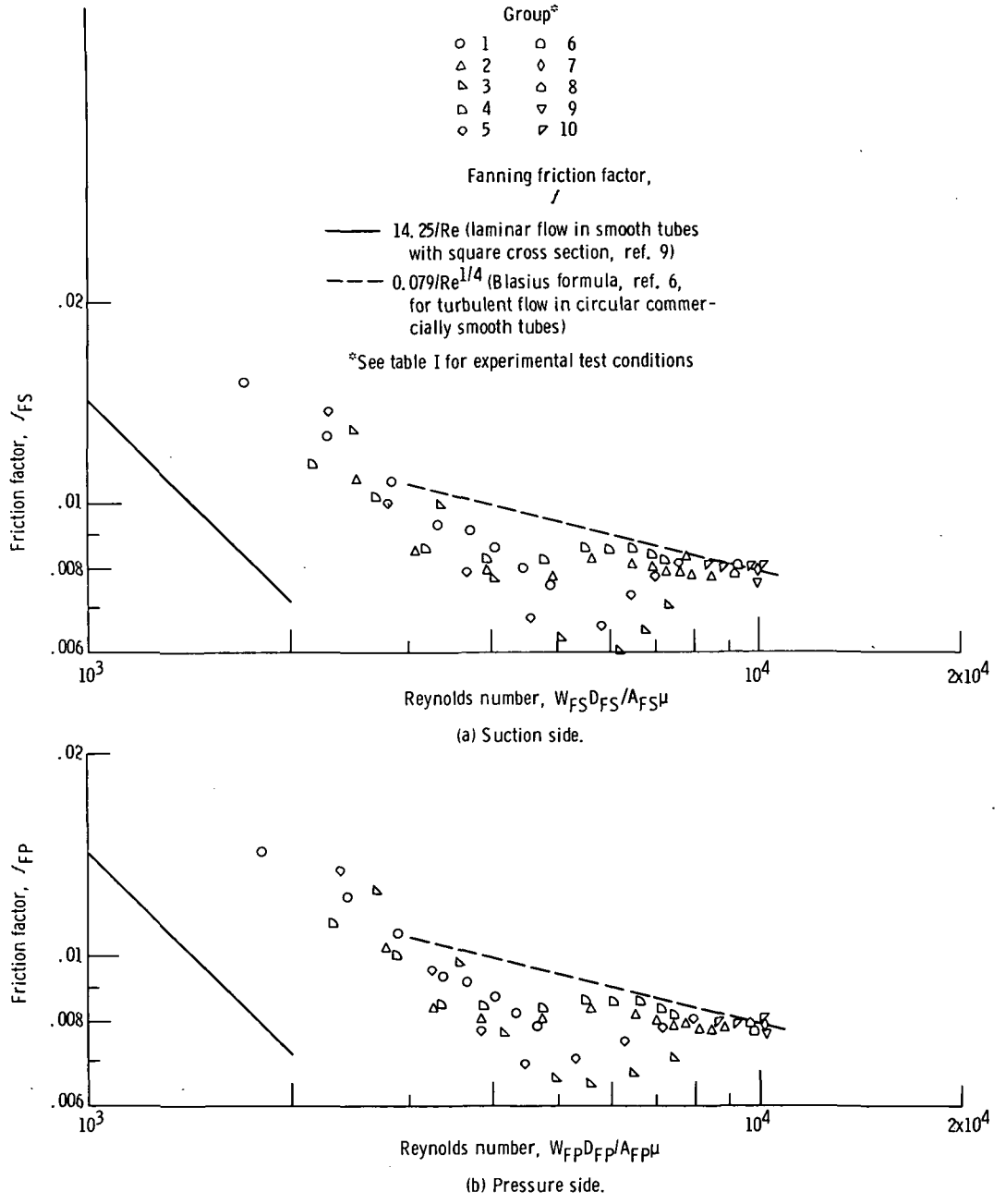

Figure 9. - Friction factors for cooling fin passages as function of cooling-fin-passage Reynolds number.

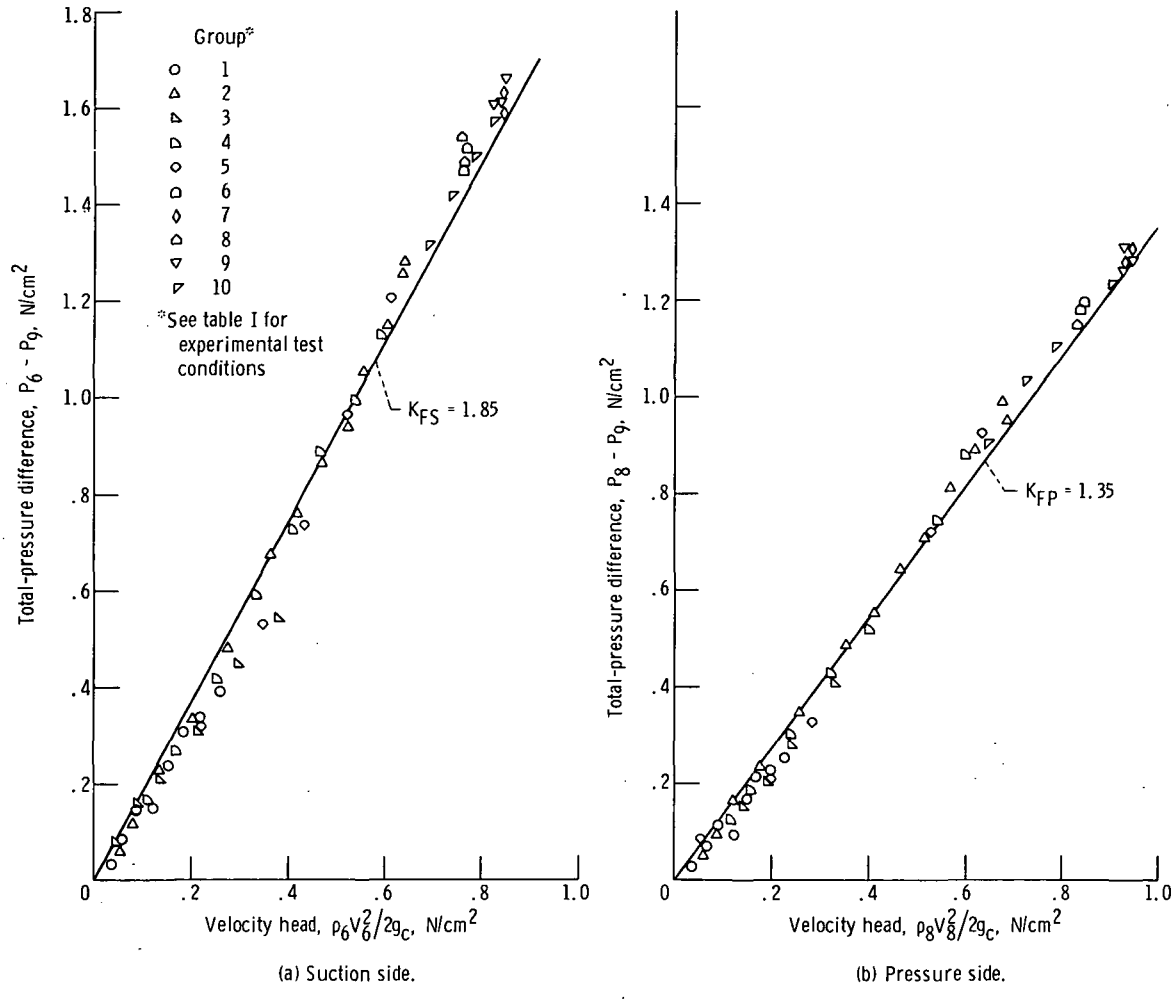

(a) Suction side.

(b) Pressure side.

Figure 10. - Cooling-fin-passage expansion loss coefficients.

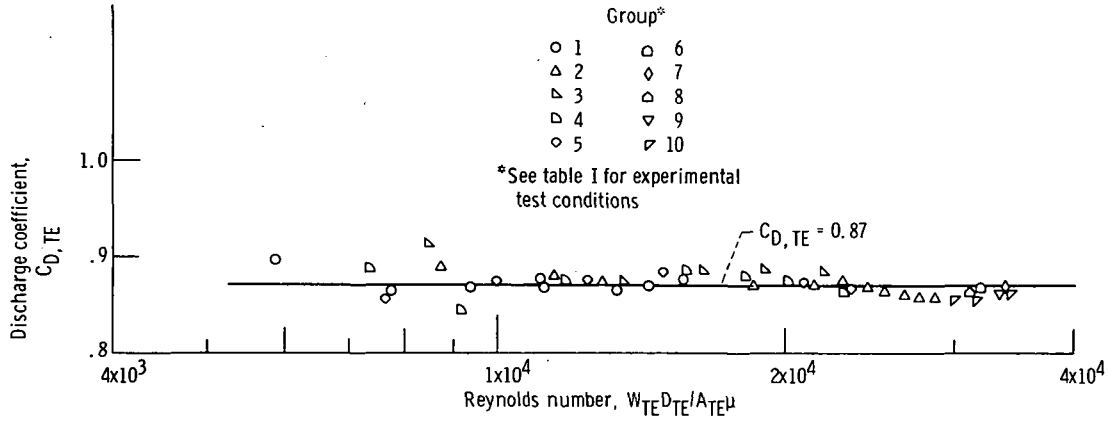

Figure 11. - Discharge coefficient for trailing-edge passage as function of trailing-edge Reynolds number.

NATIONAL AERONAUTICS AND SPACE ADMINISTRATION
WASHINGTON, D.C. 20546

OFFICIAL BUSINESS
PENALTY FOR PRIVATE USE $300

SPECIAL FOURTH-CLASS RATE BOOK

POSTAGE AND FEES PAID
NATIONAL AERONAUTICS AND SPACE ADMINISTRATION
451

U.S.MAIL

POSTMASTER: If Undeliverable (Section 158 Postal Manual) Do Not Return

"The aeronautical and space activities of the United States shall be conducted so as to contribute . . . to the expansion of human knowledge of phenomena in the atmosphere and space. The Administration shall provide for the widest practicable and appropriate dissemination of information concerning its activities and the results thereof."

—NATIONAL AERONAUTICS AND SPACE ACT OF 1958

NASA SCIENTIFIC AND TECHNICAL PUBLICATIONS

TECHNICAL REPORTS: Scientific and technical information considered important, complete, and a lasting contribution to existing knowledge.

TECHNICAL NOTES: Information less broad in scope but nevertheless of importance as a contribution to existing knowledge.

TECHNICAL MEMORANDUMS: Information receiving limited distribution because of preliminary data, security classification, or other reasons. Also includes conference proceedings with either limited or unlimited distribution.

CONTRACTOR REPORTS: Scientific and technical information generated under a NASA contract or grant and considered an important contribution to existing knowledge.

TECHNICAL TRANSLATIONS: Information published in a foreign language considered to merit NASA distribution in English.

SPECIAL PUBLICATIONS: Information derived from or of value to NASA activities. Publications include final reports of major projects, monographs, data compilations, handbooks, sourcebooks, and special bibliographies.

TECHNOLOGY UTILIZATION PUBLICATIONS: Information on technology used by NASA that may be of particular interest in commercial and other non-aerospace applications. Publications include Tech Briefs, Technology Utilization Reports and Technology Surveys.

Details on the availability of these publications may be obtained from:

SCIENTIFIC AND TECHNICAL INFORMATION OFFICE

NATIONAL AERONAUTICS AND SPACE ADMINISTRATION

Washington, D.C. 20546